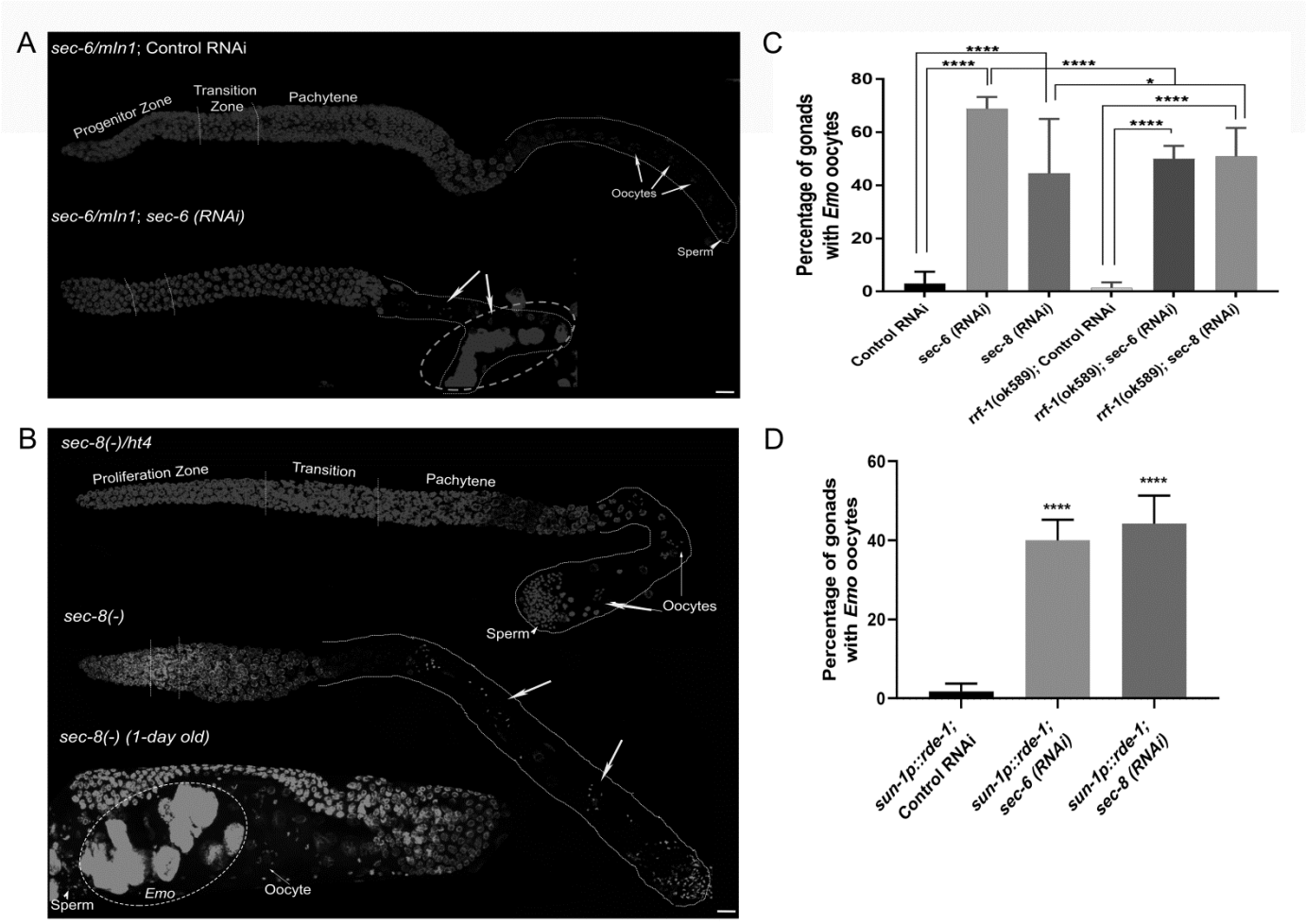

Fig. S1. Genetic mutants of sec-6 and sec-8 phenocopy RNAi-induced germline development defects. (A) Maximum projection fluorescence images of dissected and whole-mounted gonads from the indicated mutant adult genotypes, stained with DAPI (grey). **(B)** Maximum projection fluorescence images of dissected and whole mounted gonads from the indicated genotypes, stained with DAPI (grey) at young and 1-day old adult. Dashed oval marks endoreduplicating (*emo*) oocytes. For both panels: dotted vertical lines demarcate the transition zone (TZ) from the progenitor zone (PZ) and pachytene (meiotic zone); dotted trace curves outline the proximal gonadal boundary. **(C, D)** Fraction of gonads showing endoreduplicating (Emo) oocytes upon exocyst subunit RNAi in wild type (n > 80 worms) and *rrf-1* mutant worms (n >120 worms) (D) and sun-1p::rde-1 (n >100 worms). Arrows = oocytes, arrowhead = sperm. Scale bar = 20 µm.

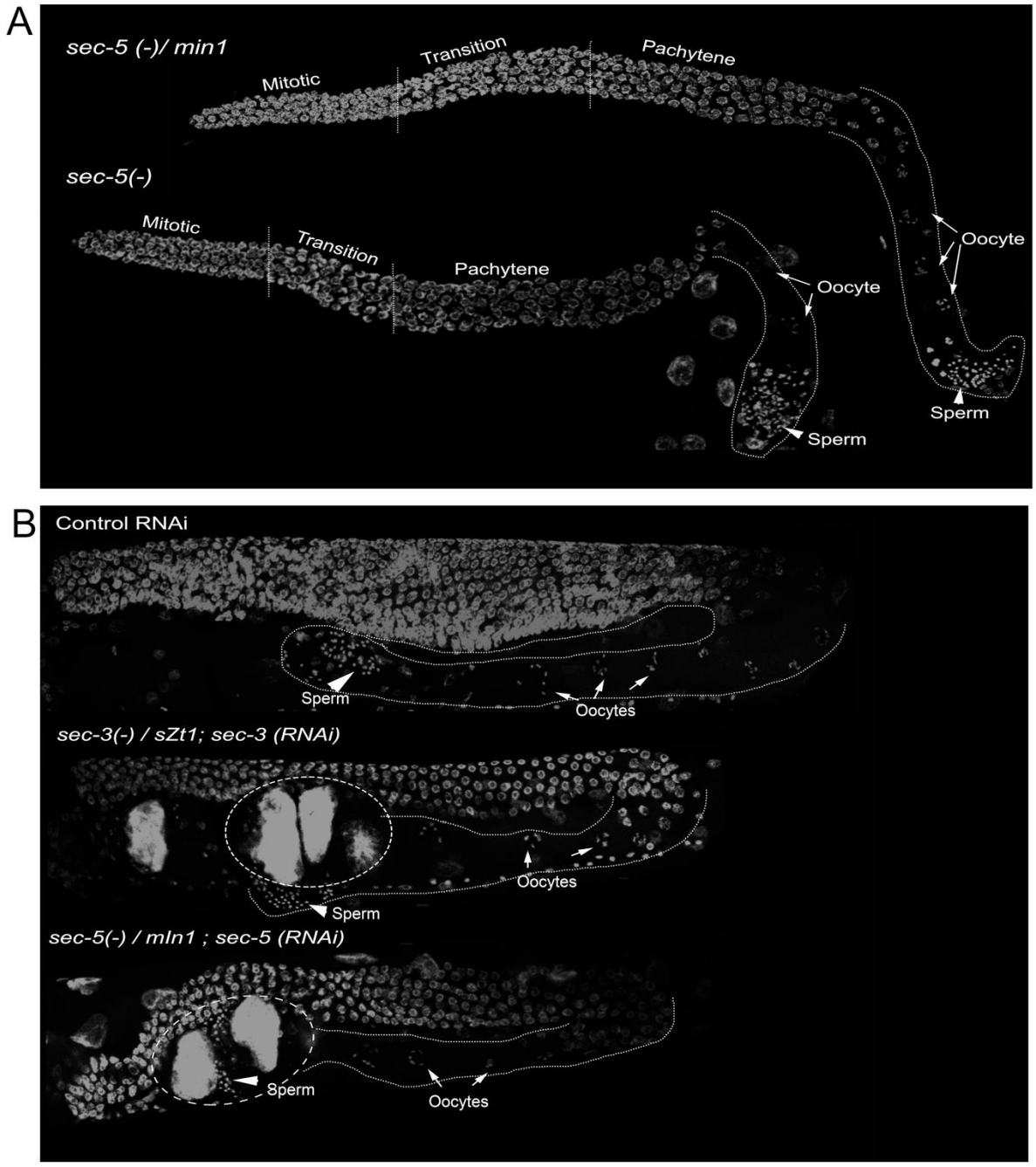

Fig. S2. Exocyst complex components sec-3 and sec-5 are required for germline development in C. elegans. (A) Maximum projection fluorescence images of dissected and whole-mounted gonads from the indicated mutant adult genotypes, stained with DAPI (grey). **(B)** Whole-mounted maximum projection images of hermaphrodite gonads stained with DAPI (grey) from the indicated genotypes. Dashed ovals mark endoreduplicating (*emo*) oocytes. For both panels: dotted vertical lines demarcate the transition zone from the progenitor zone (PZ) and pachytene (meiotic zone); dotted trace curves outline the proximal gonadal boundary. Arrows = oocytes, arrowheads = sperm. Scale bar = 20 µm

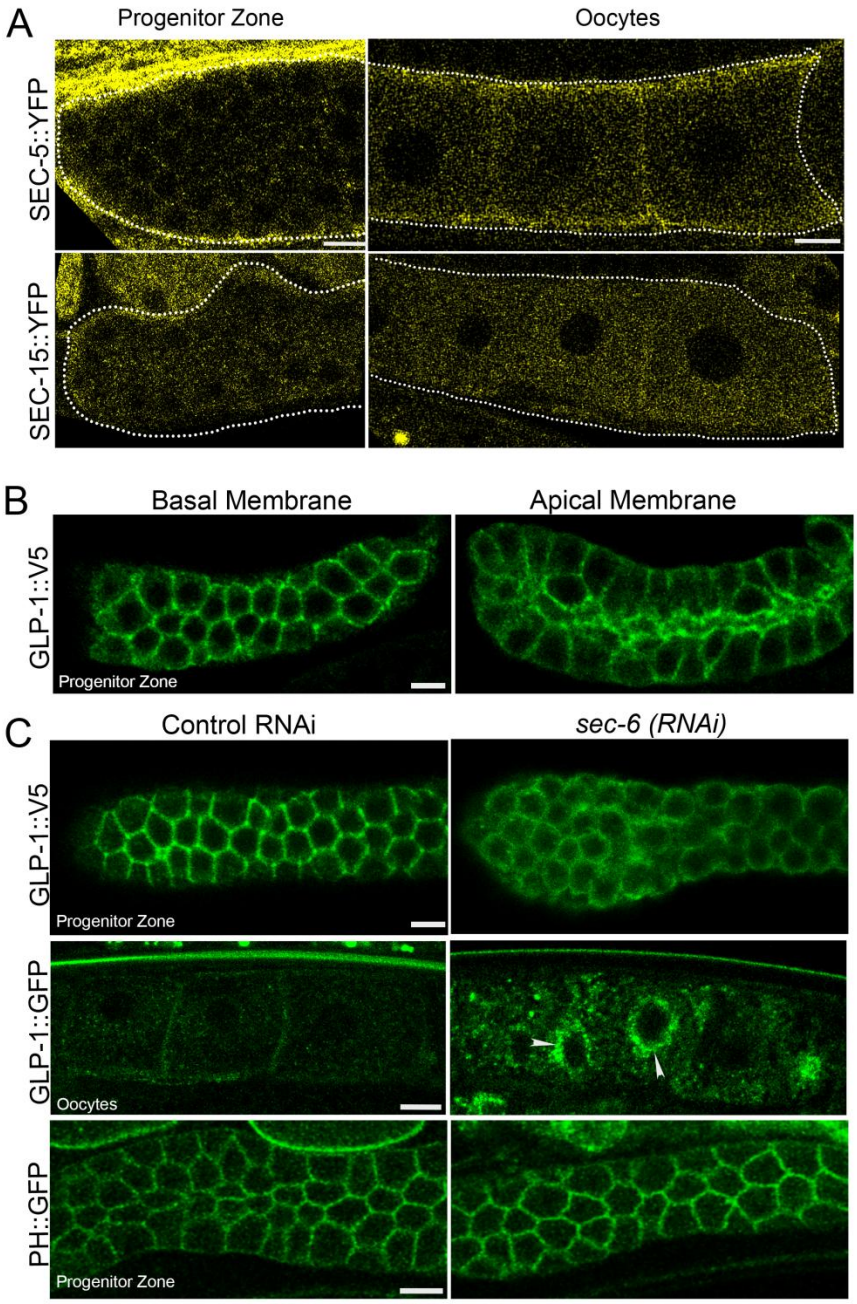

Fig. S3. The Exocyst complex is expressed in the germline and is required for trafficking of GLP-1 in the germline. (A) Representative confocal micrographs of the progenitor zone (PZ) and oocytes expressing SEC-5::YFP and SEC-15::YFP. **(B)** Representative immunofluorescence micrographs of dissected hermaphrodite gonads expressing the GLP-1::V5 transgene, stained with an anti-V5 antibody showing the outer and inner membranes (top panel) of the PZ and gonads subjected to RNAi as indicated (bottom panel). **(C)** Representative confocal fluorescence micrographs of GLP-1::V5 immunostaining on the outer membrane of GSCs (upper panel), GLP-1::GFP in oocytes (middle panel) and PH::GFP, a plasma membrane marker (bottom panel) in control and *sec-6 RNAi* Scale bar = 10 µm

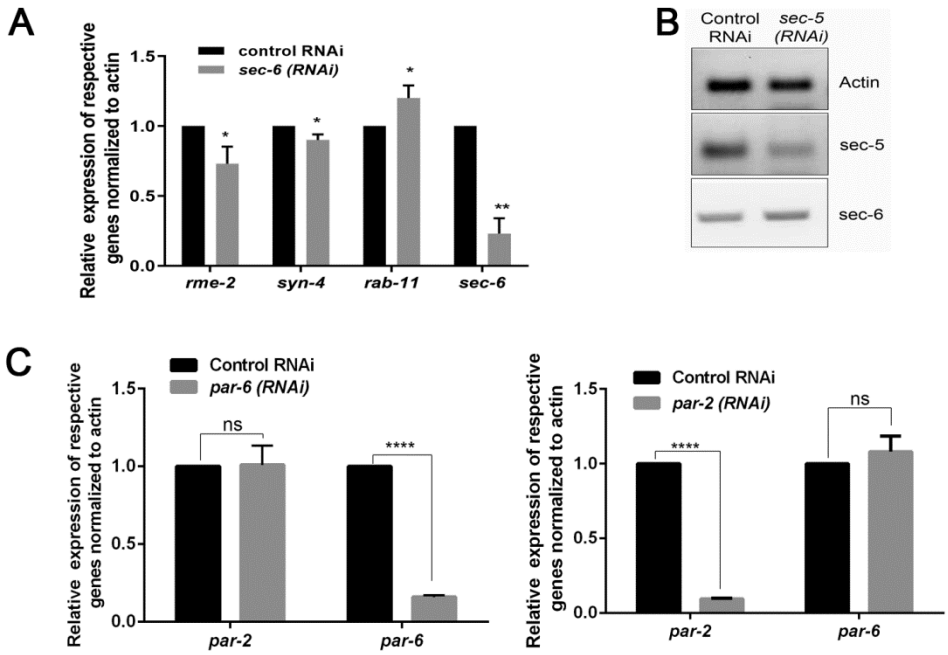

Fig. S4. A. Quantitative RT-PCR analysis of the indicated genes in the respective RNAi backgrounds. A) Relative gene expression of rme-2, syn-4, rab-11 and sec-6 upon control and sec-6 RNAi. **B))** Agarose gels showing the specific reduction in levels of the indicated genes in control and sec-5 (RNAi) using a semi-quantitative RT-PCR as compared to the β-actin control. **C)** Relative mRNA expression of par-6 and par-2 in the respective RNAi backgrounds, indicating the specificity of the RNAi.

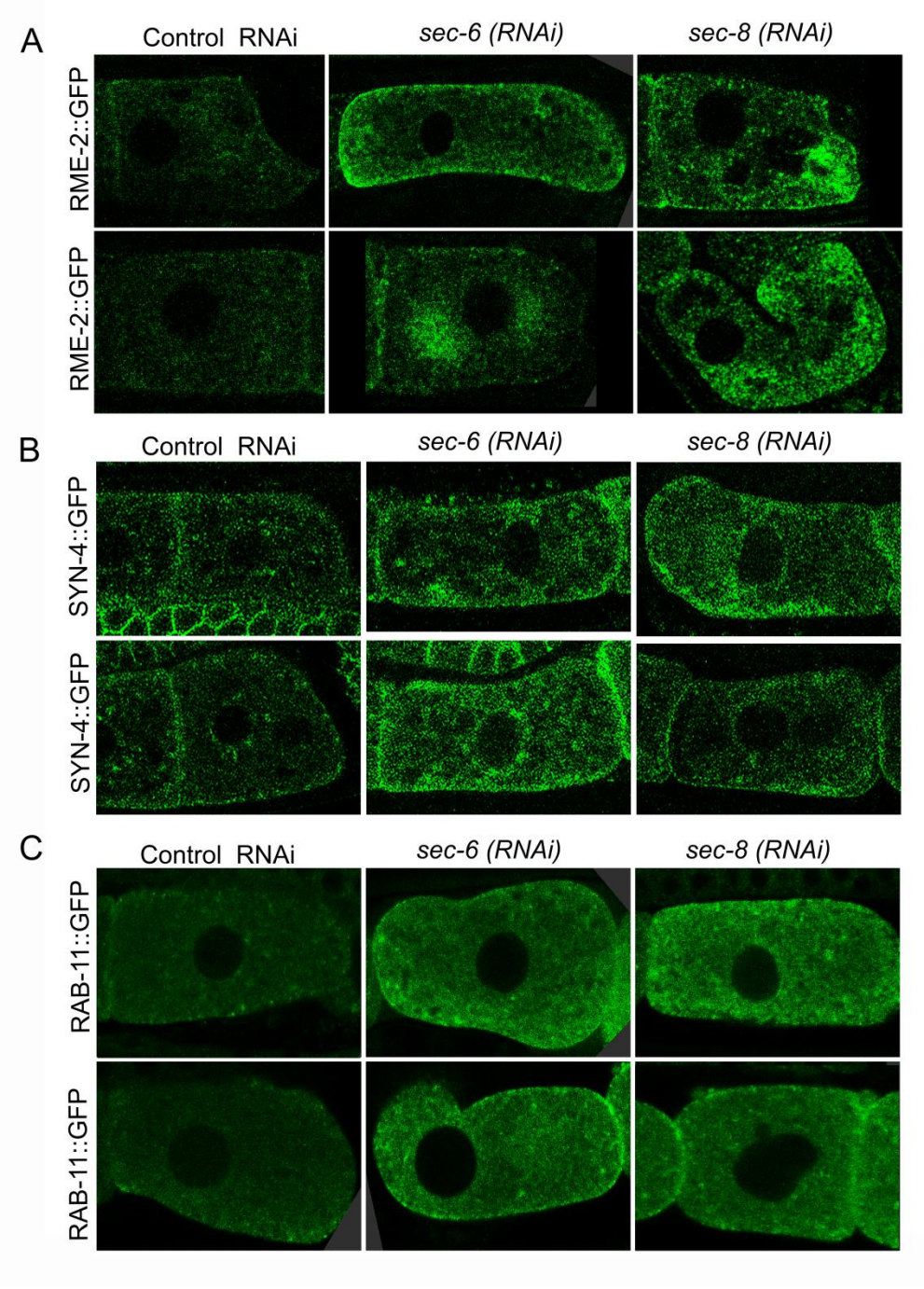

Fig. S5. The Exocyst complex is required for vesicular trafficking in C. elegans oocytes*:* Confocal fluorescence micrographs of mature oocytes expressing the indicated tagged protein RME-2::GFP **(A)**, SYN-4::GFP **(B)** and RAB-11::GFP **(C)** upon control, *sec-6* or *sec-8 (RNAi)*.

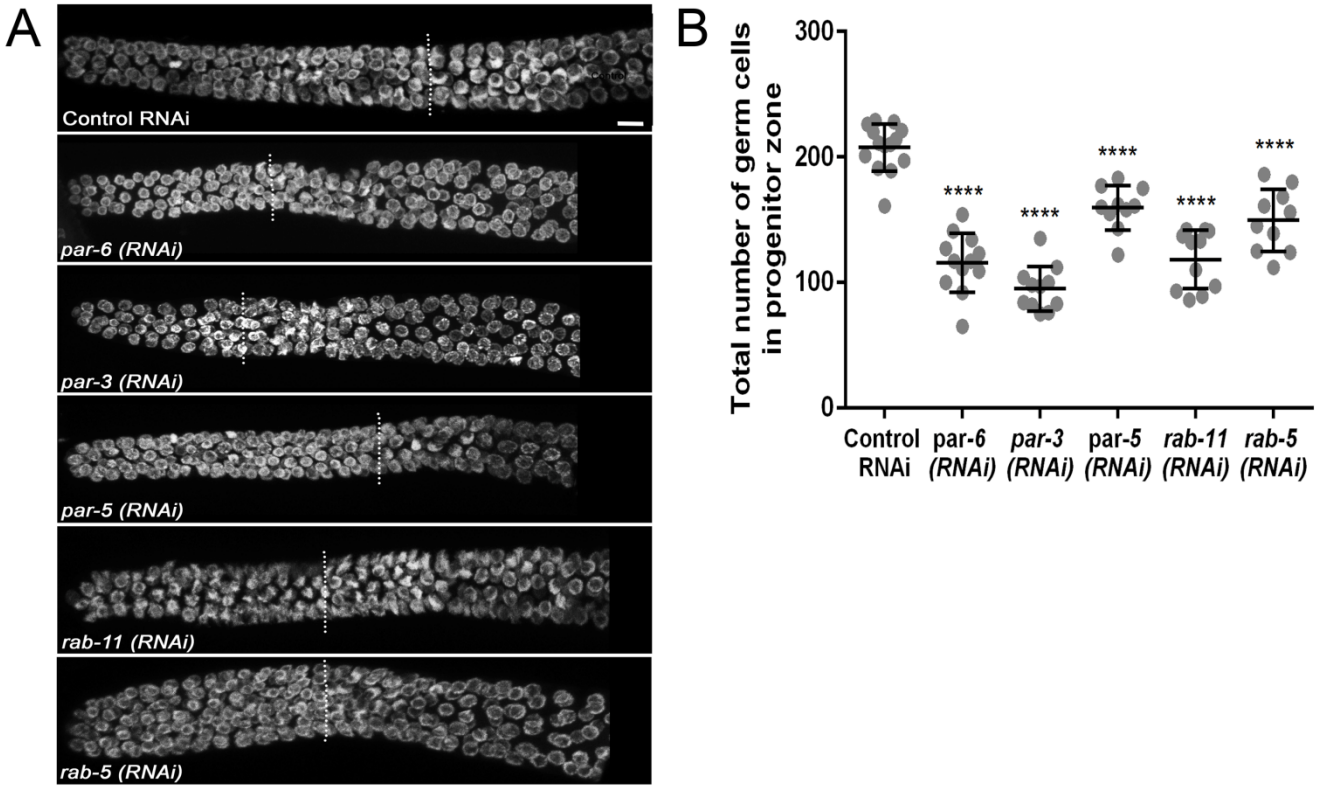

Fig. S6. Germline stem cell proliferation is defective upon RNAi of aPars and Rab GTPases Rab-5 and Rab-11: A) Representative confocal immunofluorescence micrographs of dissected hermaphrodite gonads from the indicated RNAi and stained with the DNA-binding dye (grey, DAPI). Dashed line demarcates the progenitor zone (PZ) from the transition zone (TZ). **B)** Total number of GSCs upon knockdown of the indicated genes. Scale bar = 10 µm.

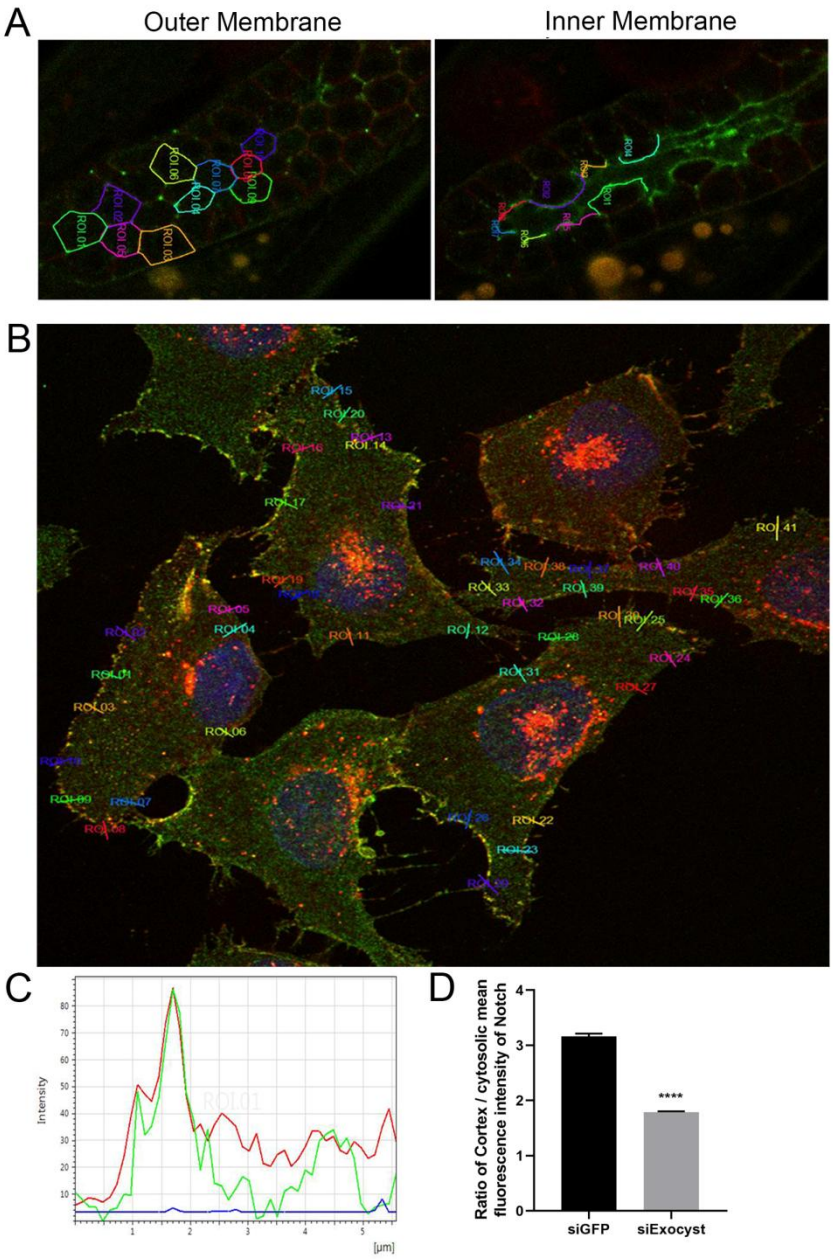

Fig. S7. Pictorial representation of methodology for drawing line scans to quantify plasma membrane levels of Notch in C. elegans and mammalian cells. **(A)** Representative micrographs of the progenitor zone (PZ) from animals expressing GLP-1::GFP (green) and PH::mCherry (red) showing the merged image (green + red). Linescans were drawn on images of a single confocal plane that corresponded to the top (for the outer surface) and middle (for the inner surface) focal plane of the gonad along the cell boundaries using red fluorescence (PH::mCherry, which decorates the plasma membrane) as a guide and the mean fluorescence intensity of the green channel (GLP-1::GFP) was calculated using LASX software analysis tool (see Materials and Methods). About 8-10 cells per gonad from 12-15 worms (one gonadal arm/worm) were used for these measurements. **(B)** Representative

max projection image of a field of mammalian cells (U2OS) co-stained with wheat-germ agglutinin (WGA – red) and human Notch2 (green). Linescans were drawn across the cell boundary from outside the cell to the cytoplasm using WGA (red) staining as the guide for the plasma membrane. Since the WGA staining was not uniform throughout, only the well-stained regions of the cell boundary were used to draw the linescans. Peak fluorescence intensity on the membrane in the green channel (for Notch2) was measured using the red channel (WGA) membrane peak as the guide. A minimum of 5 ROIs for each cell and about 40-50 ROIs per field were drawn. From a single field, only 5 cells were used for analysis to avoid over representation and uniform and unbiased data collection. **(C)** Graph shows the peak intensity at a given point on the line scan. We analyzed the peak intensity in the green channel corresponding to the plasma membrane falling within a 2 nm region of the red peak **(D)** Fraction of cortical and cytoplasmic Notch2 receptor (see Materials and Methods for details) upon control and exocyst complex siRNA treatment in U2OS cells.

A

Yeast two-hybrid		
Serial Number	Gene Name	PBS* score
1	SEC-5	**A**
2	PAR-5	**C**
3	KLC-1	**C**
4	PGL-3	**D**
5	UNC-15	**A**

PBS score: Predicted Biological Score, a confidence score attributed to interactions as described in Formstecher et al., 2005.
A: Very high confidence
B: High confidence
C: Good interaction
D. Moderate interaction
E. Highly connected interaction, due to highly interactive or connected proteins or promiscuous domains
F. Technical artifacts

B

Mass spectrometry			
Serial Number	**Gene Name**	**Number of peptides**	**% Coverage**
1	SEC-3	7	15.9
2	SEC-5	1	3.7
3	SEC-8	4	8.7
4	RAB-11	1	16.5
5	PAR-5	12	54.8
6	KLC-2	2	9.6
7	PGL-1	4	9.3
8	UNC-15	3	6.3

Fig. S8. PAR5 is identified as an interactor of exocyst subunit SEC6/ Exoc3 from C. elegans and human systems. (**A)** Selected high confidence interactors of exocyst subunit SEC-6 from *C. elegans* obtained through a yeast two-hybrid screen. See Materials and Methods for details. (**B)** Selected high confidence interactors of exocyst subunit Sec-6 from whole worm lysates expressing SEC-6::GFP::SBP, obtained through affinity purification using SBP-tag followed by mass spectrometry. See Materials and Methods for details.

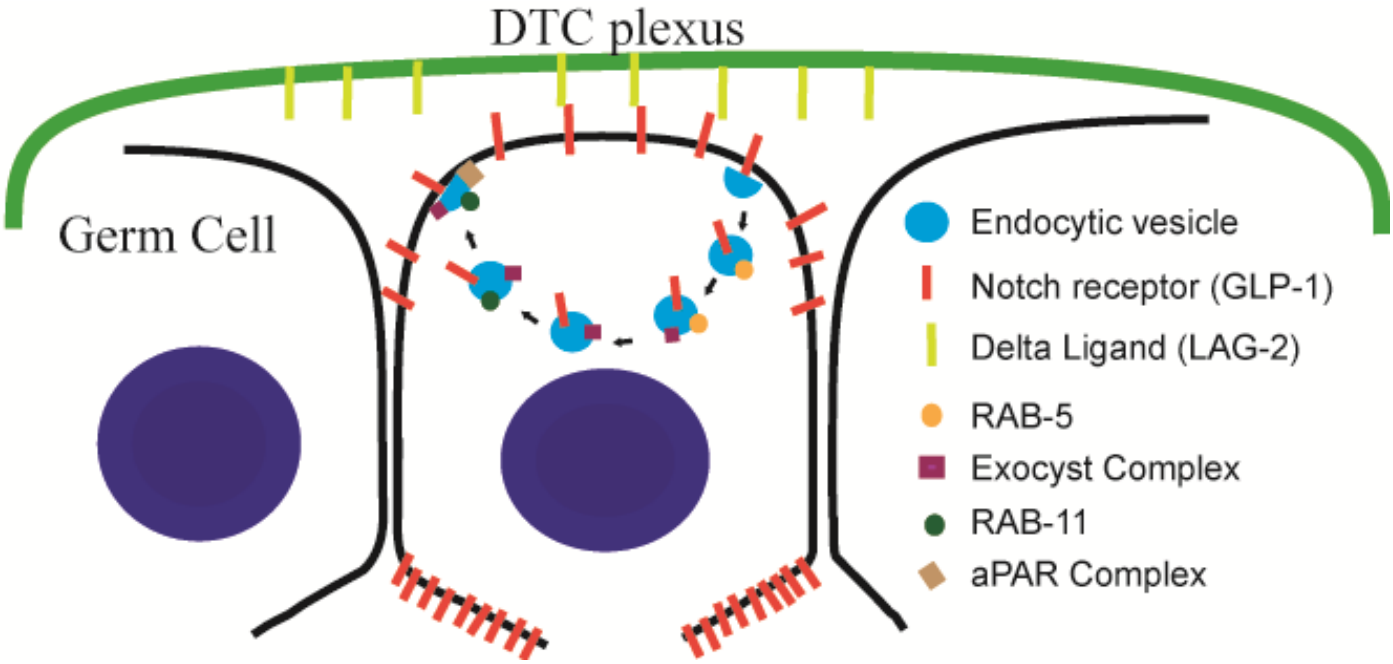

Fig. S9. Graphical model representing Notch/GLP-1 distribution in the GSCs in C. elegans and a possible mechanism of Notch trafficking and localization at the Niche-facing membrane of GSCs by Exocyst complex, Rab GTPases RAB-5, RAB-11 and aPar complex.

Table S1. Description of strains used in this study

Strain Name	Description	Source
N2	Bristol strain, Wild type	CGC
OD95	ltIs37[(pAA64) pie-1p::mCherry::his-58 + unc-119(+)] IV; ltIs38 [pie-1p::GFP::PH (PLC1delta1) + unc-119(+)]	CGC
OD70	ltIs44 [pie-1p::mCherry::PH(PLC1delta1) + unc-119(+)]	CGC
OD58	ltIs38 [pie-1p::GFP::PH(PLC1delta1) + unc-119(+)]	CGC
RT368	unc-119(ed3) III; pwIs98 [YP170::tdimer-2; unc-119 (+)]	CGC
VC2648	sec-8(ok2187) I/hT2 [bli-4(e937) let-?(q782) qIs48] (I;III)	CGC
tm4536	sec-6(tm4536) /mIn1 [mIs14 dpy-10(e128)] II	NBRP
DV2689	sec-5(pk2358)/ mIn1 [dp-10(e128) mIs14] II	CGC
VC2003	+/szT1[lon-2(e678)] I; sec-3(ok2238)/szT1 X	CGC
FT1265	sec-5(pk2358)II; xnIs461 [sec-5::YFP+ unc-119(+)]	CGC
FT1379	avr-14(ad1302) I; xnSi34 [sec-15::YFP+ Unc-119(+)] II; unc-119 (ed3) III; glc-1(pk54::Tc1) avr-15(ad1051) V	CGC
WH327	ojIs23 [pie-1p::GFP::C34B2.10]	CGC
RB798	rrf-1(ok589) I.	CGC
WH351	ojIs37 [pie-1p::GFP::ugtp-1 + unc-119(+)]	CGC
WH347	unc-119(ed3) III; ojIs35 [pie-1p::GFP::rab-11.1; unc-119 (+)]	CGC
GC833	glp-1(ar202) III	CGC
DG2389	glp-1(bn18) III	CGC
MVS1	sec-6 (SMYL04[sec-6::GFP::SBP] II	This study
MVS6	sec-6 (SMYL04[sec-6::GFP::SBP] II; ltIs44 [pie-1p::mCherry::PH (PLC1delta1) + unc-119(+)]	This study
MVS8	EV343; ltIs44 [pie-1p::mCherry::PH (PLC1delta1) + unc-119(+)]	This study
JK2868	qIs56 [lag-2p::GFP + unc-119(+)]	CGC
JH2060	axIs1498 [pie-1p::GFP::gld-1 ORF::gld-1 3'utr + unc-119(+)]	CGC
EV343	efEx12 [glp-1::TY1::EGFP::3xFLAG(92C12) + unc-119(+)]	CGC
RT408	pwIs116 [rme-2p::rme-2::GFP::rme-2 3'UTR + unc-119(+)].	CGC
JK5933	glp-1(q1000[glp-1::4xV5]) III.	Kimble Lab
JK5929	lst-1(q1004[lst-1::4XV5]) I	CGC
JK6002	sygl-1(q1004[sygl-1::4XV5]) I	CGC
MVS 10	sec-6 (SMYL04[sec-6::GFP::SBP] II; efEx12 [glp-1::TY1::EGFP::3xFLAG(92C12) + unc-119(+)]	This study
MVS 11	sec-6 (SMYL05[sec-6::degron::GFP::SBP] II	This study
CA1199	ieSi38 [sun-1p::TIR1::mRuby::sun-1 3'UTR + Cbr-unc-119(+)] IV.	CGC
MVS12	sec-6 (SMYL05[sec-6::degron::GFP::SBP] II; CA1199 (ieSi38 [sun-1p::TIR1::mRuby::sun-1 3'UTR + Cbr-unc-119(+)] IV.)	This study
DCL569	mkcSi13 [sun-1p::rde-1::sun-1 3'UTR + unc-119(+)] II.	CGC
JK2879	gld-2(q497) gld-1(q485)/hT2 [bli-4(e937) let-?(q782) qIs48] (I;III)	CGC
JK3182	gld-3(q730) nos-3(q650)/mIn1 [mIs14 dpy-10(e128)] II	CGC

Table S2. Description of oligos used in this study

Oligo name	Sequence	Purpose
PK1	TCTAAGCTTTAGCAGTCACAATCGAGCAC	Forward to clone sec-3 in RNAi vector
PK2	TCTAAGCTTCGAGAGATTGCAATTGCTCC	Reverse to clone sec-3 in RNAi vector
PK3	TCTAAGCTTACTACCTCCTACGGTAACAG	Forward to clone sec-5 in RNAi vector
PK4	TCTAAGCTTGCGTCTGCATGATTCTCTAG	Reverse to clone sec-5 in RNAi vector
PK5	TCTAAGCTTTGGACGTTGATGTGGAAGAG	Forward to clone sec-6 in RNAi vector
PK6	TCTAAGCTTGAACTTCGGCCAGCAATTCG	Reverse to clone sec-6 in RNAi vector
PK7	TCTCCCGGGCTAGAAGGCATCGACCATTG	Forward to clone sec-8 in RNAi vector
PK8	TCTCCCGGGTCCACTCGTGATAATCGTCC	Reverse to clone sec-8 in RNAi vector
MVS136	TCCGAGAATCTTCCTAATTGAAAT	Forward to detect rrf-1(ok589) deletion
MVS138	TCGAAGGGATTCAATTCGTC	Reverse to detect rrf-1(ok589) deletion
PK17	GTGGAACAAATGCCGATGAG	Forward to detect sec-6(tm4536) deletion
PK38	TCTGAGGGATCCATGGACGTTGATGTGGAAGAG	Forward to detect sec-6(tm4536) deletion
MVS395	AACTTCAAAATTAGACACAACATTGAAGAT	Forward to detect SEC-6::GFP Crisper-edit
MVS396	AGTCAGCTTTGAACATGTTGGC	Reverse to detect SEC-6::GFP Crisper-edit
MVS393	CAGACACAGATGTTCCGTTG	Fwd in Sec-5(pk2358) ahead of mutation
MVS392	GAGAAAAGTCTCTGGGATATGT	Fwd to detect Sec-5(pk2358) mutant
MVS394	GAAGAGCTTTGGGAACCAG	Reverse to detect mutation in sec-5(pk2358)
MVS389	GTACTGGGAACTGCAAGCAG	Forward to detect Sec-8 deletion
MVS390	GCAGGAGAAGACAAGAATCAGC	Fwd to detect Sec-8 deletion
MVS499	AAGCTGGTGTCGCGTGTATG	Forward for rme-2 RT-PCR
MVS500	ATGACTCCAGCGAATGGTGC	Reverse for rme-2 RT-PCR
MVS508	CTCTCGTGACGATGAATACGAC	Forward for rab-11.1 RT-PCR
MVS509	CACTGTCTTGCCTTCTACCG	Reverse for rab-11.1 RT-PCR
MVS510	CGCAGATCGACACGCAATTT	Forward for syn-4 RT-PCR
MVS511	ATGCCACGTGCTTGAGCTAT	Reverse for syn-4 RT-PCR
MVS512	CGGAGAGGAGCAAGTATCAAGAG	Forward for Sec-6 RT-PCR
MVS513	TACGTCGTCCTGATGCGAGT	Reverse for Sec-6 RT-PCR
MVS514	CGTTTTGGAGATCCGCTCAG	Forward for Sec-8 RT-PCR
MVS515	TCTGCTTGCAGTTCCCAGTA	Reverse for Sec-8 RT-PCR
MVS516	CGATTCGTGATGTGTGTGCT	Forward for Par-2 RT-PCR
MVS517	GGTGATGACGTGGGAGTTTG	Reverse for Par-2 RT-PCR
MVS518	TTCTCGGAAAGACGCTGGAT	Forward for Par-6 RT-PCR
MVS519	GCTGAATTCCACCTGTAGCG	Reverse for Par-6 RT-PCR
MVS520	CCGCTCTTGCCCCATCAACCATG	Forward for actin RT-PCR
MVS521	CGGACTCGTCGTATTCTTGCT	Reverse for actin RT-PCR
MVS534	GGCTCTCTCAACGTATGCCA	Forward for Sec-5 RT-PCR
MVS535	TCGCATAGTGGTTCGCATGT	Reverse for Sec-5 RT-PCR
MVS522	GGCTGTGGCCGAAGTGAT	Forward for hExoc3 RT-PCR
MVS523	CTGGATACTTGGCGTCCCC	Reverse for hExoc3 RT-PCR
MVS526	CGAGGTGGAGAAGGAGAGTG	Forward for Hey1 RT-PCR
MVS527	CTGGGTACCAGCCTTCTCAG	Reverse for Hey1 RT-PCR
MVS530	AACTGTTGGTGGCCTGAATC	Forward for Herp2 RT-PCR
MVS531	GCTGGTAAATGCAGGCGTAT	Reverse for Herp2 RT-PCR

Table S3

Click here to download Table S3